MNRAS **000**, 1–6 (2016) Preprint 9 February 2017 Compiled using MNRAS LATEX style file v3.0

Temporal intensity interferometry for characterization of very narrow spectral lines

P. K. Tan[1⋆], and C. Kurtsiefer[1,2†]
[1] *Centre for Quantum Technologies, 3 Science Drive 2, 117543, Singapore*
[2] *Department of Physics, National University of Singapore, 2 Science Drive 3, 117551, Singapore*

ABSTRACT
Some stellar objects exhibit very narrow spectral lines in the visible range additional to their blackbody radiation. Natural lasing has been suggested as a mechanism to explain narrow lines in Wolf-Rayet stars. However, the spectral resolution of conventional astronomical spectrographs is still about two orders of magnitude too low to test this hypothesis. We want to resolve the linewidth of narrow spectral emissions in starlight. A combination of spectral filtering with single-photon-level temporal correlation measurements breaks the resolution limit of wavelength-dispersing spectrographs by moving the linewidth measurement into the time domain. We demonstrate in a laboratory experiment that temporal intensity interferometry can determine a 20 MHz wide linewidth of Doppler-broadened laser light, and identify a coherent laser light contribution in a blackbody radiation background.

Key words: Instrumentation: Interferometers – Line: Identification – Techniques: Spectroscopic

1 OBSERVED NARROW EMISSION LINES

Spectral emission lines have been observed in stellar systems, such as Wolf-Rayet stars, Be stars, T Tauri stars, P Cygni and luminous blue variables (Kogure & Leung 2007; van der Hucht 2001).

One example is the Wolf-Rayet progenitor SN2013cu, which exhibited emission lines (Gal-Yam et al. 2014) with relatively broad base of 2500 km/s Full Width at Zero Intensity (FWZI) on which narrow unresolved (limited at 150 km/s) lines are superimposed.

Another candidate is the η Car stellar system, where emission lines (Hamann 2012) were observed from the Weigelt knots that are separated from the host star by only about 0.3 ". Ground based spectroscopy has seeing-limited angular resolution of around 1 ", and is thus unable to spatially resolve the spectral contributions by the Weigelt knots from the star and the surrounding Homunculus Nebula.

Observations by the Hubble Space Telescope which could spatially resolve the Weigelt knots from the rest of the η Car system found emission lines (Zethson et al. 2012) with spectral widths limited by the instrument resolution of 0.05 nm (corresponding to velocity spreads of 25 km s^{-1}).

⋆ pengkian@physics.org (PKT)
† phyck@nus.edu.sg (CK)

2 THEORETICAL ASTROPHYSICAL LASERS

This suggests either very low temperatures of the emission medium, or a different mechanism like stimulated emission (Schawlow & Townes 1958), which can lead to optical emission much narrower than the participating atomic or molecular transition. Following first laboratory demonstrations of maser and laser radiation and the detection of strong interstellar microwave emission from molecular gas clouds (Weaver et al. 1965), natural non-visible lasers from astrophysical sources were proposed to be responsible for this emission (Menzel 1970; Varshni & Nasser 1986).

Natural stellar laser candidates in the visible range are expected to have a spectral linewidth around 10 MHz (Johansson & Letokhov 2005) that cannot be easily resolved by conventional astronomical spectrographs. Therefore, alternative spectroscopical techniques like heterodyne spectroscopy (Hale et al. 2000; Sonnabend et al. 2005) or, as we investigate in this paper, temporal photon correlation spectroscopy may help to better understand the nature of these narrow emission lines.

3 COMPARISON WITH OTHER SPECTROSCOPY TECHNIQUES

Modern astronomical echelle spectrographs have typical resolutions between 30,000 to 150,000 (Murphy et al. 2007), with the target starlight and reference calibration light (such as laser frequency combs) fed by multi-mode fibres, because starlight cannot be efficiently coupled to single-mode optical fibres in the visible regime (Wilken et al. 2012).

Optical homo- or heterodyning (Siegman 1966; Mandel & Wolf 1975) has the potential for a basically unlimited spectral resolution, but is conditional on the overlap of spatial modes between the input light with the local oscillator. While this can be accomplished in lab environment using single mode fibres, it is inefficient to couple starlight into optical single-mode fibres due to atmospheric **turbulence and seeing** (Fried 1967). Mode matching in a free space geometry for heterodyning is equally difficult for the same reason (Shaklan & Roddier 1988).

For Michelson interferometry or Fourier transform spectroscopy, which could be less sensitive to phase fluctuations, a resolution of tens of MHz would require scanning a path length difference over several meters in steps shorter than the optical wavelength (Loewenstein 1966; Sakai et al. 1968) – a requirement that would be mechanically very challenging.

Temporal photon correlation spectroscopy is in widespread use in material science and fluorescence microscopy, where it is also referred to as dynamic light scattering and quasi-elastic light scattering, and used to characterise the particle distribution in suspensions (Saleh 1978; Becker 2005; Pike 2010). Application of this spectroscopy technique in astronomy seems less common (Dravins & Germanà 2008), but may be advantageous in characterizing narrow line widths. Moreover, one may even be able to experimentally assess the presence of a natural lasing mechanism in the visible range directly, as we show in this work.

4 INTENSITY INTERFEROMETRY FOR TIME DOMAIN SPECTROSCOPY

Intensity interferometry was used to investigate the spatial coherence properties of starlight to infer their angular diameter (Hanbury-Brown & Twiss 1956), but first demonstration experiments were carried out on spectral lines from a Mercury gas discharge lamp (Hanbury-Brown & Twiss 1958). In essence, normalized intensity correlations

$$g^{(2)}(\tau) = \frac{\langle I(t)I(t+\tau)\rangle}{\langle I(t)\rangle^2} \tag{1}$$

are recorded as a function of the time difference τ by evaluating photodetection events from detectors observing the same light source. For stationary light of a single polarization, the normalized intensity correlation $g^{(2)}(\tau)$ is related to the normalized (electrical) field correlation $g^{(1)}(\tau)$ (Mandel & Wolf 1995) via

$$g^{(2)}(\tau) = 1 + |g^{(1)}(\tau)|^2 \,. \tag{2}$$

The Wiener-Khinchin theorem (Wiener 1930; Khinchin 1934) links the field correlation to the spectral power density $S(f)$ through a Fourier transform $\mathcal{F}$:

$$S(f) \propto \mathcal{F}[g^{(1)}(\tau)] \,. \tag{3}$$

Therefore – within the limits of reconstructing the phase of the complex $g^{(1)}(\tau)$ from $g^{(2)}(\tau)$ via (2) – it is possible to extract information about the spectral power density $S(f)$ of the light source from a measured intensity correlation $g^{(2)}(\tau)$. A narrow spectral distribution $S(f)$ of width δf will result in a $g^{(2)}(\tau)$ with a characteristic time scale $\tau_c \propto 1/\delta f$.

The width δf of narrow spectral lines can therefore be measured in the time domain, overcoming the resolving power of wavelength-dispersive instruments like spectrographs or narrow-band interference filters. Note, however, that this does not allow determination of the absolute spectral position of a line, since a frequency shift Δf of a narrow distribution results in a complex oscillating term $e^{2\pi i \Delta f \tau}$ in $g^{(1)}(\tau)$, but leaves $g^{(2)}(\tau)$ unchanged due to the modulus in (2).

In stellar light sources, narrow spectral lines tend to appear against a large background of blackbody radiation. A direct measurement of the second order correlation function is therefore difficult, because the signal is dominated by the blackbody contribution with a very short coherence time on the order of 10^{-14} s. Therefore, adequate preliminary filtering has to suppress the thermal background to a level that time domain spectroscopy can be carried out. It is also necessary that the light exhibits some non-Poissonian intensity fluctuations, since for light with Poissonian statistics, e.g. coherent laser light, the intensity correlation is flat ($g^{(2)}(\tau) = 1$) (Glauber 1963) and has no structure that would reveal any spectral properties.

In this work, we simulate the characteristic spectrum of natural stellar laser candidates in the visible range by combining phase-randomized artificially Doppler-broadened laser light with spectrally wide blackbody radiation. We then characterize the narrow spectral line by time-resolved intensity interferometry after passing the composite light through a diffraction grating and two etalons to suppress the blackbody contribution.

5 EXPERIMENTAL SETUP

Our experimental setup is illustrated in Fig. 1. Composite test light is prepared by combining light from a laser diode (Osram PL520, $P = 50\,\mathrm{mW}$) at a wavelength of λ_L=513.8 nm with blackbody radiation from an Argon arc lamp with an effective blackbody temperature of around 6000 K on an uncoated microscope glass slide. This combines approximately 4 % of the incident laser light with 92 % of the Argon arc lamp output, **with another 4 % loss in the splitter due to lack of anti-reflective coating**. The resulting spectrum recorded with a grating spectrometer of approximately 0.12 nm resolution is shown in Fig. 2.

The very narrowband laser light is Doppler-broadened by passing it through a cuvette containing a suspension of standard mono-disperse polystyrene microspheres of 0.2 μm diameter in water, following Dravins et al. (2015). These microspheres serve as scattering centers undergoing Brownian motion at room temperature. The resultant phase randomization causes the laser light to exhibit pseudo-thermal photon bunching behavior (Martienssen & Spiller

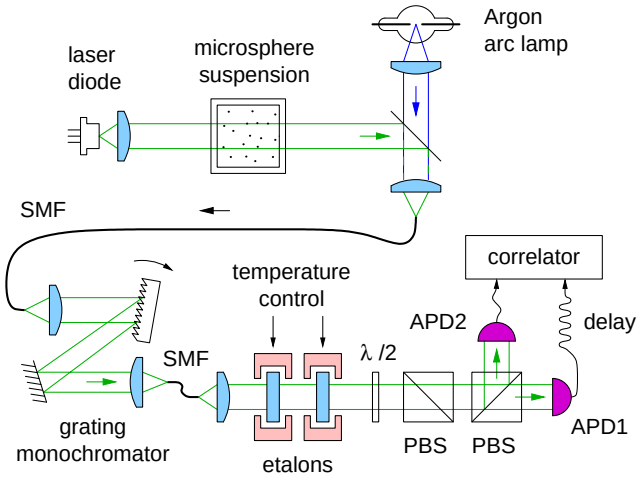

Figure 1. Experimental setup. Light from a laser diode (λ_L = 513.8 nm) is Doppler-broadened by passing through a suspension of microspheres (0.2 μm diameter), combined with light from an Argon arc lamp on a microscope slide, and coupled into a single mode optical fiber (SMF). The bottom part shows the analysis system, consisting of a grating monochromator and a temperature-tuned etalon pair to select a 3.2 GHz wide spectral window around 513.8 nm from the composite light. Temporal photon pair correlations are recorded to identify different light contributions. PBS: polarizing beam splitter, $\lambda/2$: half wave plate, APD: single photon avalanche photodetectors.

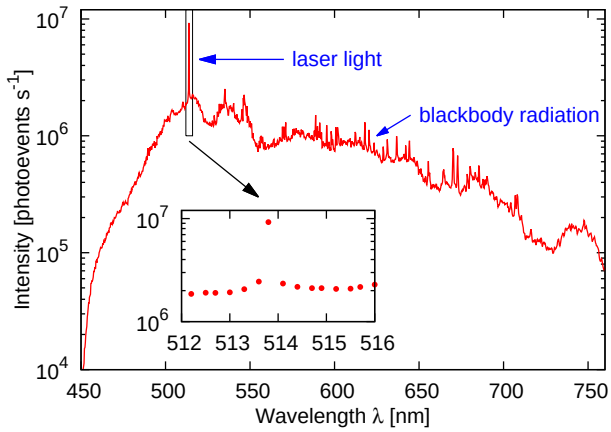

Figure 2. Spectrum of the test light source in Fig. 1 without Doppler broadening. The broad background over the whole visible range resembles blackbody radiation at an effective temperature T = 6000 K, while the inset shows the unresolved spectrum around the laser line. The resolution of the spectrometer is about 0.12 nm.

1964; Arecchi 1965; Scarl 1966, 1968; Estes et al. 1971; Hard et al. 1977). The coherence properties of light leaving the suspension depend on the temperature of the suspension, the viscosity (ratio of water to microspheres), and beam focus (Dravins & Lagadec 2014); these parameters were not fully characterized, but a combination of a beam waist of roughly 1 mm, with beads-concentration of approximately 0.1% solids [weight/volume] at room temperature (23 degrees Celsius) lead to Doppler-broadened light we could investigate with our technique.

The microsphere suspension with its milky appearance reduces the intensity of the laser light by over two orders of magnitude, which is too low to allow proper identification against the blackbody radiation background in a spectral measurement with our grating spectrometer.

To identify the laser light admixture to the blackbody radiation, the test light is first coupled into a single mode fibre (Thorlabs 460HP). After collimation, the light passes through a monochromator based on a reflective diffraction grating (1200 lines/mm, blazed for 500 nm). The monochromator is calibrated to the 546.1 nm line from a Mercury discharge lamp where it shows a transmission bandwidth (full width at half maximum, FWHM) of about 0.12 nm.

A second single mode fiber enforces spatial coherence again, before the light passes through a pair of temperature-tuned plane-parallel solid etalons made of fused silica (Suprasil311) with a refractive index n=1.4616, and coatings of a nominal reflectivity $R = 95.2\,\%$ at λ_L. This corresponds to an estimated finesse $\mathcal{F}_R = \pi\sqrt{R}/(1-R) = 63.9$. The etalons have thicknesses of d_1=0.5 mm and d_2=0.3 mm, corresponding to a free spectral range FSR $= c/(2dn)$ of 205 GHz and 342 GHz, respectively. Their temperatures are stabilized to overlap the transmission maxima at the laser wavelength. Both etalons, in conjunction with the diffraction grating, suppresses most of the blackbody background (Tan et al. 2014), transmitting only an optical bandwidth $\delta f \approx \mathrm{FSR}_1/\mathcal{F}_R \approx 3.2$ GHz (FWHM), corresponding to a coherence time $\tau_c = 1/\delta f \approx 0.31$ ns. This filter combination has an effective spectral resolving power fo about 10^5, which is comparable to current astronomical spectrographs (Griest et al. 2010).

The filtered light is polarized by a first polarizing beam splitter (PBS), and distributed by a second PBS into a pair of actively quenched Silicon avalanche photodetectors (APD) with a timing jitter of about 40 ps (Tan et al. 2016). Photodetection rates are balanced by rotating the first PBS which is preceeded by a half wave plate to maximize the count rates. Coincidence photoevents are recorded using a fast digital oscilloscope. The photodetectors exhibit a dark count rate of 50 events/sec, predominantly from the detector thermal noise, which is negligible in the subsequent coincidence measurements. The coincidence histograms were normalized to obtain a $g^{(2)}(\tau) = 1$ for large τ, because the oscilloscope had an unknown dead time for histogram processing that made a direct normalization impossible.

6 IDENTIFYING EMISSION LINEWIDTH

In a first experiment, we want to measure the linewidth of the laser light that was Doppler-broadened by random scattering in the microsphere suspension on a background of blackbody radiation. Both broadened laser light and blackbody radiation resulted in about 2×10^4 photoevents per second each behind the filter stack formed by gratings, etalons and polarization filters.

The histogram of two-photon coincidences as a function of photodetection event separation τ is shown in Fig. 3, with a total of 2×10^6 coincidences recorded for -2 ns $< \tau <$ 96 ns. For time differences $|\tau|$<1 ns, the sharp peak due to filtered blackbody radiation is visible, while on a longer time scale, the Doppler-broadened laser contribution due to phase ran-

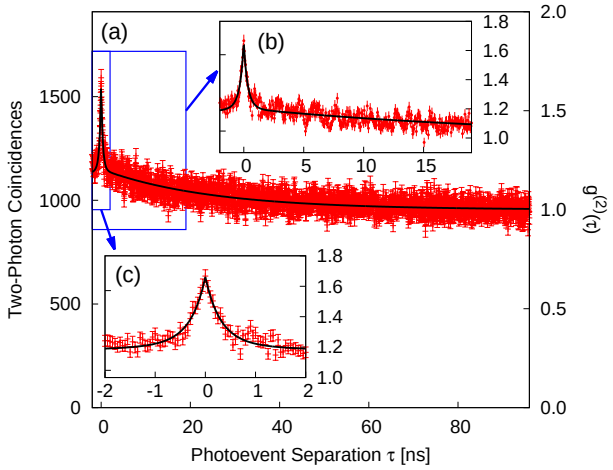

Figure 3. (a) The two-photoevent coincidence histogram from filtered blackbody radiation with a Doppler broadened laser light contribution shows two exponential decays on a short and a long time scale (bin width 50 ps). The solid line shows a fit of the data to model (8), assuming $f_B = f_L$. The two zooms show (b) an oscillatory behaviour on top of the slow decay, and (c) a good match between the fit and the measured data for the filtered blackbody radiation on a short time scale.

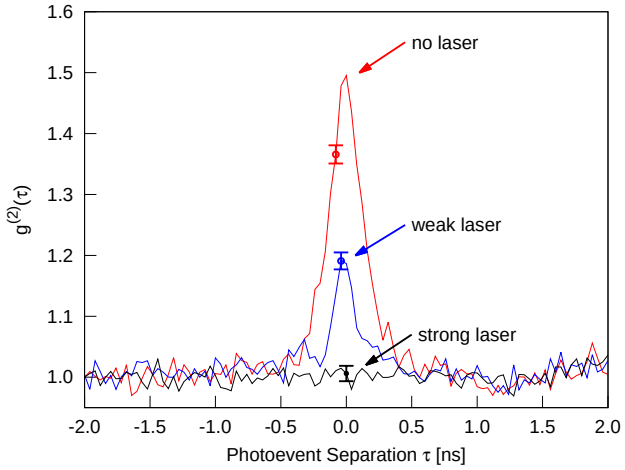

Figure 4. Temporal photodetection correlations for different ratios of coherent laser and filtered blackbody radiation: all measurements have a blackbody contribution of approximately 3×10^4 photoevents/sec. For the "strong laser" trace, the laser contributed about 6×10^6 photoevents/sec, for the "weak laser" trace about 3×10^4 photoevents/sec. For reference, the photodetection correlations of filtered blackbody radiation without any laser light is also shown. Each measurement accumulated 10^6 coincidence photoevents with -3.1 ns< τ <3.3 ns into 40 ps wide bins to allow for direct comparison of the resulting histograms. The error bars reflect Poissonian counting statistics and are representative for all time differences. Fitting the "no laser" trace to model (5) leads to a coherence time τ_c=0.31±0.01 ns, and to τ_c=0.26±0.03 ns for the trace with a weak laser.

domization in the microsphere suspension leads to photon bunching with a slower decay constant.

A single Lorentzian frequency distribution

$$S(f) = \frac{\sqrt{a}}{\pi}\frac{\delta f/2}{(f-f_0)^2+(\delta f/2)^2} \tag{4}$$

around a center frequency f_0 with a linewidth (FWHM) of δf leads via (2) and (3) to a normalized correlation function

$$g^{(2)}(\tau) = 1 + a e^{-|2\tau|/\tau_c} \quad \text{with} \quad \tau_c = 1/\delta f\,. \tag{5}$$

For a mixed spectral distribution $S(f)$, the intensity correlation function $g^{(2)}(\tau)$ can be obtained in a similar way. If the two contributions from blackbody and laser light are assumed to be mutually incoherent, the spectral power densities $S_B(f)$ and $S_L(f)$ can be added,

$$S(f) = S_B(f) + S_L(f)\,, \tag{6}$$

and the resulting intensity correlation is given by

$$g^{(2)}(\tau) = 1+|g^{(1)}(\tau)|^2 = 1+\left|\mathcal{F}^{-1}\left[S_B(f)\right]+\mathcal{F}^{-1}\left[S_L(f)\right]\right|^2\,, \tag{7}$$

with $\mathcal{F}^{-1}$ indicating the inverse Fourier transform. Assuming now two Lorentzian distributions $S_B(f)$ and $S_L(f)$ according to (4) with amplitudes a_L, a_B, coherence times τ_B, τ_L, and center frequencies f_L, f_b, respectively, the Fourier transformation can easily be carried out, leading to

$$\begin{aligned} g^{(2)}(\tau) &= 1+\left|a_B e^{-|\tau|/\tau_B}+a_L e^{-|\tau|/\tau_L}\right|^2 \\ &= 1+a_B^2 e^{-|2\tau|/\tau_B}+a_L^2 e^{-|2\tau|/\tau_L} \\ &\quad +2\cos[2\pi(f_L-f_B)\tau]\,a_B a_L\, e^{-|\tau|(1/\tau_B+1/\tau_L)}\,. \end{aligned} \tag{8}$$

For $f_L = f_B$, the oscillating term vanishes, and (8) becomes a sum of three exponential decays on top of $g^{(2)} = 1$ that can readily explain the correlation function in Fig. 3. There, the decay for large τ is dominated by the larger coherence time τ_L. The small peak near $\tau = 0$ is a combination of two fast decays, one given by the correlation of the blackbody contribution alone, the other one by the mixed term with about twice the decay time for $\tau_L \gg \tau_B$. A fit of the observed correlation function to the model (8) over photoevent separations of $-2\,\text{ns} < \tau < 96\,\text{ns}$ leads to $\tau_B = 0.39 \pm 0.03$ ns, $\tau_L = 49.0 \pm 2.3$ ns, $a_B = 0.36 \pm 0.02$, and $a_L = 0.452 \pm 0.004$. However, the relatively large reduced variance $\chi^2_{\text{red}} = 1.26$ indicates that model (8) is too simple, and does e.g. not capture the oscillatory contributions in the measured $g^{(2)}$ visible in Fig. 3(b). The long coherence time corresponds to a linewidth of $\delta f = 1/\tau_L \approx 20$ MHz, comparable to the ones predicted for natural stellar lasers.

The described technique thus allows linewidth measurements of extremely narrow spectral lines, limited only by the ability to record a sufficiently large number of photons to construct a coincidence histogram. The upper bound of a linewidth measurement with this technique is given by the time resolution of the photodetectors and time-tagging mechanism (in our case a few GHz). However, the phase uncertainty of $g^{(1)}(\tau)$, if inferred from $g^{(2)}(\tau)$ in (2), requires further assumptions for a direct reconstruction of a spectrum via (3).

7 IDENTIFYING COHERENT LIGHT

In a second experiment, we try to identify the presence of coherent laser emission by a quantitative evaluation of the photobunching signature $g^{(2)}(\tau = 0)$. For this, we remove the microsphere suspension, and record the temporal corre-

lation measurement for different admixture levels of attenuated laser radiation to a blackbody radiation background of about 3×10^4 photoevents/sec after the filter stack. Assuming a Lorentzian spectral distribution (4), the fit of the observed second order correlation leads to a a coherence time τ_c=0.31±0.01 ns, in agreement with τ_B obtained from the fit in the first experiment.

The results are shown in Fig. 4. Without any laser light contribution, a detector-limited blackbody temporal bunching signature of approximately $g^{(2)}(0) = 1.5$ is observed, compatible with the transmission bandwidth around 3.2GHz of the etalon stack at λ_L central wavelength and the timing jitter of the avalanche photodetectors (Tan et al. 2016).

For a weak laser contribution ($\approx 10^4$ photoevents/sec) on top of a blackbody background, the temporal photon bunching signal is reduced to $g^{(2)}(0) \approx 1.2$, indicating a sub-thermal photon bunching signature. This means that even the presence of small contributions of coherent light is revealed by the reduction of the thermal photon bunching signature expected from the filtered blackbody component.

For the third trace in Fig. 4, the laser light contribution is over two orders of magnitude stronger than the filtered blackbody contribution, corresponding to the power ratio used to obtain the spectrum in Fig. 2. The timing correlation appears constant within the statistical uncertainty, without an observable temporal photon bunching signature from the blackbody contribution.

The last trace resembles a typical photodetection correlation observed photodetectors exposed to wide-band radiation, like in the traditional experiments of Hanbury-Brown & Twiss (1958), but with a significant difference: since the optical bandwidth of the detected radiation is narrower than the inverse detector timing uncertainty, the *reduction* of a photobunching signal can be interpreted as a signature of a light source with sub-thermal statistics, e.g. due to contributions of coherent light from a lasing mechanism.

8 CONSIDERATIONS FOR SPECTROSCOPY OF ASTROPHYSICAL CANDIDATES

Precision spectroscopy of astronomical objects is often limited by the Signal-to-Noise Ratio (SNR) of a particular technique. To compare the photocorrelation spectroscopy with other techniques, we consider the SNR of temporal intensity interferometry due to propagated Poissonian photon statistics for a narrowband emission line as described by (Hanbury-Brown 1974; Malvimat et al. 2013):

$$SNR = \tau_c \frac{r}{2} V(b)^2 \sqrt{\frac{\Delta T}{2\Delta t}}\,. \tag{9}$$

In this expression, τ_c is the coherence time of the emission line with a lower bound provided by the spectral bandpass, r the photodetection rate, ΔT the overall measurement duration, Δt the electronic resolution constrained by the photodetectors, and $V(b)$ the spatial visibility over baseline separation b, which approaches $V = 1$ for a telescope aperture much smaller than the transverse stellar coherence length.

The observed visible emission lines from η Car have intensities on the order of 10^4 photons m^{-2} s^{-1} (Mehner et al. 2010; Dravins & Germanà 2008). To achieve a SNR of 3 with the spectral filtering technique described in this paper with a 3 GHz bandpass and detectors with 40 ps timing jitter, collecting starlight with a telescope of about 0.4 m aperture would require an observation time of approximately 6 hours. In contrast, using a conventional interference filter with 1 nm bandpass would correspondingly increase the telescope aperture to about 7 m for the same SNR in 6 hours.

While tuning of the etalons by temperature leads to a very good short term stability for the prefilters, it is still fast enough (i.e., within a few minutes) to account for time-dependent Doppler shifts of about 0.7 GHz light in the visible range due to the daily motion of the earth with respect to an astronomical object, or about 50 GHz due to the Earth's motion around the Sun.

9 SUMMARY

Time-resolved second order correlation spectroscopy was used to identify the presence of very narrow-band light on a thermal background. The linewidth of pseudo-thermal light could be determined that was generated by phase-randomization in a multiple scattering process, similar to light from an ensemble of emitters without a fixed phase relationship, like a gas cloud excited by a nearby star. Temporal intensity interferometry offers a spectral resolution of at least a few 10 MHz for emission lines, exceeding by far that of contemporary astrophysical spectrographs.

Also, an identification of sub-thermal photon statistics can be carried out with the presented technique indicating a possible optical lasing mechanism, and therefore help to better understand the very narrow spectral features of stellar light sources even in presence of a strong blackbody radiation background.

ACKNOWLEDGEMENTS

We acknowledge the support of this work by the National Research Foundation and the Ministry of Education in Singapore, partly through the Academic Research Fund MOE2012-T3-1-009.

REFERENCES

Arecchi F. T., 1965, Phys. Rev. Lett., 15, 912
Becker W., 2005, Advanced Time-Correlated Single Photon Counting Techniques. Springer-Verlag Berlin Heidelberg, doi:10.1007/3-540-28882-1
Dravins D., Germanà C., 2008, in Phelan D., Ryan O., Shearer A., eds, The Universe At Sub-Second Timescales. AIP, USA, p. 284
Dravins D., Lagadec T., 2014, Proc. SPIE, 9146, 91460Z
Dravins D., Lagadec T., Nunēz P. D., 2015, Nat. Commun., 6, 6852
Estes L. E., Narducci L. M., Tuft R. A., 1971, J. Opt. Soc. Am., 61, 1301

Fried D. L., 1967, Proceedings of the IEEE, 55
Gal-Yam A., et al., 2014, Nature, 509
Glauber R., 1963, Phys. Rev., 131, 2766
Griest K., Whitmore J. B., Wolfe A. M., Prochaska J. X., Howk J. C., Marcy G. W., 2010, ApJ, 708, 158
Hale D. D. S., et al., 2000, ApJ, 537
Hamann F., 2012, Eta Carinae and the Supernova Impostors. Springer, pp 95–128, doi:10.1007/978-1-4614-2275-4_5
Hamann F., DePoy D. L., 1994, ApJ, 422, 626
Hanbury-Brown R., 1974, The Intensity Interferometer: Its Application To Astronomy. Taylor & Francis ; Halsted Press, London ; New York
Hanbury-Brown R., Twiss R. Q., 1956, Nature, 178, 1046
Hanbury-Brown R., Twiss R. Q., 1958, Proc. Roy. Soc., 243, 291
Hard R., Zeh R., Allen R. D., 1977, J. Cell Sci, 23, 335
Johansson S., Letokhov V. S., 2005, New Astronomy, 10, 361
Khinchin A., 1934, Mathematische Annalen, 109, 604
Kogure T., Leung K.-C., 2007, The Astrophysics of Emission-Line Stars. Springer-Verlag New York, doi:10.1007/978-0-387-68995-1
Loewenstein E. V., 1966, Applied Optics, 5, 845
Malvimat V., Wucknitz O., Saha P., 2013, MNRAS, 437, 798
Mandel L., Wolf E., 1975, JOSA, 65
Mandel L., Wolf E., 1995, Optical Coherence and Quantum Optics. Cambridge University Press
Marco O. D., Schmutz W., Crowther P., Hillier D., Dessart L., de Koter A., Schweickhardt J., 2000, A&A, 358, 187
Martienssen W., Spiller E., 1964, Am. J. Phys, 32, 919
Mehner A., Davidson K., Ferland G. J., Humphreys R. M., 2010, ApJ, 710, 729
Menzel D. H., 1970, in Groth H. G., Wellmann P., eds, Proceedings of IAU Colloquia No.2 Commission 36 Vol. 332, Spectrum Formation in Stars with Steady-State Extended Atmospheres. p. 134
Murphy M. T., et al., 2007, MNRAS, 380, 839
Pike E. R., 2010, JEOS:RP, 5, 10047S
Roche P. F., Colling M. D., Barlow M. J., 2012, MNRAS, 427, 581
Sakai H., Vanasse G. A., Forman M. L., 1968, JOSA, 58, 84
Saleh B., 1978, Photoelectron Statistics: With Applications to Spectroscopy and Optical Communication. Springer-Verlag Berlin Heidelberg
Scarl D. B., 1966, Phys. Rev. Lett., 17, 663
Scarl D. B., 1968, Phys. Rev., 175, 1661
Schawlow A. L., Townes C. H., 1958, Phys. Rev, 112, 1940
Shaklan S., Roddier F., 1988, Applied Optics, 27, 2334
Siegman A. E., 1966, Proceedings of the IEEE, 54
Sonnabend G., Wirtz D., Vetterle V., Schieder R., 2005, A&A, 435, 1181
Tan P. K., Yeo G. H., Poh H. S., Chan A. H., Kurtsiefer C., 2014, ApJ, 789, L10
Tan P. K., Chan A. H., Kurtsiefer C., 2016, MNRAS, 457, 4291
Varshni Y. P., Nasser R. M., 1986, Astrophysics and Space Science, 125, 341
Weaver H., Williams D. R., Dieter N., Lum W., 1965, Nature, 208, 29
Wiener N., 1930, Acta Mathematica, 55, 117
Wilken T., et al., 2012, Nature, 485, 611
Zethson T., Johansson S., Hartman H., Gull T. R., 2012, A&A, 540
van der Hucht K. A., 2001, New Astronomy Reviews, 45, 135

This paper has been typeset from a TEX/LATEX file prepared by the author.